Supplementary Online Material

Organo-mineral interactions and soil carbon mineralizability with variable saturation cycle frequency

Angela R. Possinger[a‡], Scott W. Bailey[b], Thiago M. Inagaki[c], Ingrid Kögel-Knabner[c,d], James J. Dynes[e], Zachary A. Arthur[e], Johannes Lehmann[a,d,f]

[a] *School of Integrative Plant Science, Section of Soil and Crop Sciences, Cornell University, Ithaca, NY 14853, USA*
[b] *US Forest Service Northern Research Station, North Woodstock, NH 03262, USA*
[c] *Chair of Soil Science, Technical University Munich, 85354 Freising, Germany*
[d] *Institute for Advanced Study, Technical University Munich, 85748 Garching, Germany*
[e] *Canadian Light Source, Saskatoon, SK S7N, 2V3, Canada*
[f] *Cornell Atkinson Center for Sustainability, Cornell University, Ithaca, NY 14853, USA*

** Corresponding Author. Email: CL273@cornell.edu*

‡ Present address: Virginia Tech, 220 Ag-Quad Ln, Blacksburg, VA 24061, USA, Email: arp264@vt.edu

1. Supplementary Methods

1.1 Carbon composition of organic horizon water extracts

Water extractions were done with a composite of Oa horizons from 3 replicate profiles for high and low saturation frequency soil units. Extractions were conducted at a 1:1 w/v soil (wet weight) to water ratio with overnight shaking, following by 30 min centrifugation at 12,000 rpm. Water-extractable organic matter (WEOM) extracts were filtered to 0.45 µm (Whatman GF/A glass fiber filters) and stored at < 9°C until used for characterization analysis. The carbon (C) composition of WEOM extracts was determined using C K-edge X-ray absorption near edge structure (XANES) spectroscopy. Measurements were conducted at the high-resolution spherical grating monochromator (SGM) end station of the Canadian Light Source (CLS). Samples were prepared by thin-layer deposition of ~60 µL DOM on gold (Au)-coated silicon wafers and air-drying. Partial fluorescence yield (PFY) scans (60s) were collected with an ~50 x 50 µm probe in slew mode. The PFY with maximum C signal (detector 90° to incident beam) was normalized to the PFY scattering signal from a clean Au-coated Si wafer to account for in-line C contamination. For samples and standards, 32 and 10 scans were collected from a new spot on the sample and averaged, respectively.

1.2 Carbon XANES peak height ratio determination

Carbon K-edge XANES spectra for organic horizon extracts and all subsequent C XANES analyses (manuscript section 2.3.3) (bulk soils, particulate organic matter, and bulk soil extractions with water) were flattened and normalized (edge step=1) in Athena (Demeter 0.9.25) (Ravel and Newville, 2005). Composition was assessed by comparing

peak height ratios of the 3 primary spectral features: aromatic (C=C) at ~285.0 eV, substituted aromatic (e.g., C=C-OH) at ~286.5 eV, and carboxylic (C=O-OH) at ~288.7 eV (Solomon et al., 2009; Heymann et al., 2011). Peak heights were determined by the Gaussian function fitting algorithm in Fityk v. 1.3.1 (Wojdyr, 2010), identifying the maximum of a Gaussian function of full-width half maximum (FWHM) = 0.6 eV within the defined ranges of 283.75-286.1 eV for aromatic C, 286.0-287.0 eV for substituted aromatic C, and 288.0-289.5 eV for carboxylic C (Solomon et al., 2009, Heymann et al., 2011).

1.3 Basic soil characterization

Soil pH in 0.01 M calcium chloride ($CaCl_2$) was determined with air-dry soil at a 1:2 v/w soil ratio (Hendershot et al., 1993). Total C and total nitrogen (N) were determined by combustion with a Carlo-Erba NC2500 elemental analyzer (CE Instruments Ltd, Wigan, UK). Total metals were measured using the lithium (Li) meta/tetraborate flux method (Kurtz et al., 2000). Ball-milled, ashed (550°C) soils were reacted with a 1:1 mixture of Li-metaborate and Li-tetraborate added at a 4:1 flux reagent:soil ratio. Ashed soils were also used to determine loss-on-ignition (LOI) of SOM. The mixture was fused at 1050°C for 1 h, followed by dissolution of the fusion bead in 10% nitric acid (HNO_3). Extracted metals were analyzed in a 2% nitric acid matrix using a SpectroBlue inductively-coupled plasma optical emission spectrometry (ICP-OES) instrument (Ametek, Kleve, Germany).

1.4 Metal selective extractions

All selective extract metal contents were determined with ICP-atomic emission spectrometry (ICP-AES) (Thermo iCAP 6500 series, ThermoFisher Scientific, Bellafonte, PA) in a 2% nitric acid matrix. All soil samples were air-dried and ball-milled to a fine powder prior to extractions.

1.4.1 Acid ammonium oxalate. Organically-complexed, non-crystalline and semi-crystalline metals were measured by acid ammonium oxalate (0.2 M ammonium oxalate ($(NH_4)_2C_2O_4$) with 0.2 M oxalic acid ($H_2C_2O_4$) adjusted to pH 3) extraction at a 1:40-60 soil:extractant ratio (Ross and Wang, 1993; Shang and Zelazny, 2008). Acid ammonium oxalate may also effectively extract crystalline Mn oxides, and extract minor amounts of crystalline Fe and Al oxides (including magnetite, Fe_2O_4), crystalline Mn, and structural Fe and Al in trioctahedral aluminosilicates (Parfitt and Childs, 1988; Shang and Zelazny, 2008). The extraction was completed in the dark with additional filtration (low-phosphate Whatman 512 1/2, Whatman Inc., North Bend, OH) prior to centrifugation (20 min at 1000 rpm). The optical density of the oxalate extract (ODOE) was determined by absorbance at 430 nm using a Shimadzu UV-Vis 2600 (Shimadzu Corp., Kyoto, Japan).

1.4.2 Hydroxylamine-HCl. Organically-complexed, non-crystalline, and semi-crystalline metals were determined by hydroxylamine-hydrochloric acid (HCl) extraction (Ross and Wang, 1993; Shang and Zelazny, 2008). Hydroxylamine-HCl may also extract minor amounts of lepidocrocite and maghemite (Shang and Zelazny, 2008). For all mineral soil horizons, the extraction was completed at a 1:250 w/v soil:extract ratio using 0.25 M

hydroxylamine-HCl in 0.25 M HCl (pH ~2). Supernatant aliquots were centrifuged at 11,500 rpm for 10 min prior to ICP analysis.

1.4.3 Citrate-dithionite. Organically complexed, poorly crystalline, and crystalline but non-aluminosilicate or rock metal phases were extracted using citrate-dithionite (Parfitt and Childs, 1988; Ross and Wang, 1993). Soils were extracted at a 1:25 to 1:50 w/v soil:extract ratio with 0.4 g solid sodium dithionite ($Na_2S_2O_4$) in 0.68 M sodium citrate ($Na_3C_6H_5O_7$). Filtration was completed prior to centrifugation (Whatman 595 1/2) at 2000 rpm for 30 min.

1.5 Random Forest modeling

Mineral soil characterization data were randomly split into training and testing sets (75 and 25%, respectively) and a training data model constructed with the Random Forest algorithm using an out-of-bag bootstrapping approach (100X resampling), and the following parameters: (1) node size = 5, (2) maximum number of trees (ntree) = 500, and number of variables per level (mtry) = 2. The model included 16 parameters (pH, horizon type, horizon depth, saturation frequency, dithionite-extractable Fe and Al, oxalate- and hydroxylamine-extractable Fe, Al, and Mn, and total Fe, Al, and Mn) and was independently computed 5 times with unique training and testing sets to assess model stability in variable importance rankings. Eluvial horizon identity and high saturation frequency served as reference levels for horizon type and saturation frequency categorical variables, respectively. A simple linear model of predicted and observed C contents was used to assess model predictive ability.

1.6 Mineral soil carbon K-edge XANES

Soil samples were air-dried, sieved to 2 mm, and ball-milled to a fine powder. Approximately 10 mg of soil was suspended in 500 μL DI water and vortexed briefly (10 s). Water-extracted OM (WEOM) from mineral soils was freeze-dried and finely pulverized. Due to the low volume of solid phase material in WEOM, all freeze-dried residue was re-suspended in 50 μL DI water and vortexed for ~60 s to ensure suspension homogeneity. For all suspensions, ~60 μL suspension was deposited as a thin layer on Au-coated silicon wafers and air-dried. Carbon K-edge PFY spectra were collected for 40-60 point scans (probe size 50x50 μm) in slew mode (>100 μm spacing), and interpolated and averaged using the SGM Laboratory Analysis and Acquisition System GUI. A fluorescent line peak of 290.0 eV (width 100.0 eV) ROI was used. Energy position was calibrated by alignment of the carboxylic acid peak of a citric acid standard (288.70 eV). The maximum scattering signal of an Au-coated silicon wafer was used for incidence flux normalization. Spectra were processed and peak heights determined as described in Supplementary Methods Section 1.2.

1.7 Carbon K-edge XANES damage test

Potential spectral artifacts arising from beam damage were assessed by collecting 20 sequential spectra at a fixed point for a high-C (low saturation frequency) and low-C (high saturation frequency) bulk soil sample (Supplementary Fig. A10). Directional change in fine structure ratios over time was considered evidence of beam damage, as well as the appearance of new features over time. Due to spectral noise of individual scans, 5 scans were interpolated and averaged to generate 4 time points (5, 10, 15, and

20 s). Spectra were processed and peak heights determined as described in Supplementary Methods Section 1.2.

1.8 ^{13}C Nuclear magnetic resonance Fe interference calculations

A line broadening (smoothing) value of 75 was used for all samples and ^{13}C-NMR spectra. For each soil sample, 6 spectra were collected with contact times of 0.03, 0.25, 0.5, 1, 2, 3, and 4 ms, respectively. Spectra were integrated using the following C functional group regions: alkyl C (0 to 45 ppm), O/N alkyl C (45 to 110 ppm), aromatic C (110 to 160 ppm), and carboxylic C (160 to 220 ppm) (Knicker and Lüdemann, 1995). The $\log_{10}$-transformed signal intensity of each region was plotted as a function of contact time (Preston et al., 1984) (Supplementary Fig. A9). The slope of the line from 0.5-4 ms (linear component) was converted to $T_{1\rho}H$ (^{1}H relaxation time) by the formula:

Eq. 1: Slope = *-1/* $T_{1\rho}H$ (Preston et al., 1984)

2. Supplementary Results and Discussion

2.1 Organic horizon water extract composition

Water-extractable OM from higher and lower saturation frequency soil organic horizons was similar in composition, with a slight increase in carboxylic/aromatic C ratio (18%) in high saturation frequency organic horizon extracts (Supplementary Fig. A2). The increase in carboxylic/aromatic ratio is attributed to an increase in height of the aromatic peak (rather than increase in the carboxylic peak) at low saturation frequency (Supplementary Fig. A2).

2.2 Carbon K-edge XANES damage test

Though peak height ratios were variable across the 20 min measurement period, no directional or systematic changes were detected, suggesting variability may be due to low signal/noise of averaged scans rather than beam damage (Supplementary Fig. A10). Additionally, no systematic increase of a new spectral feature was identified over time (Supplementary Fig. A10).

REFERENCES

Berry, A.J., O'Neill, H.St.C., Jayasuriya, K.D., Campbell, S.J., Foran, G.J., 2003. XANES calibrations for the oxidation state of iron in silicate glass. Am. Mineral. 88(7), 967-977.

Chen, C., Dynes, J.J., Wang, J., Sparks, D.L., 2014. Properties of Fe-organic matter associations via coprecipitation versus adsorption. Environ. Sci. Technol. 48, 13751-13759.

Hendershot, W.H., Lalande, H., Duquette, M., 1993. Soil reaction and exchangeable acidity, in: Carter, M.R (Ed.), Soil Sampling and Methods of Analysis. Canadian Society of Soil Science, Lewis Publishers, Boca Raton, pp. 141-145.

Heymann, K., Lehmann, J., Solomon, D., Schmidt, M.W.I., Regier, T., 2011. C 1s K-edge near edge X-ray absorption fine structure (NEXAFS) spectroscopy for characterizing functional group chemistry of black carbon. Org. Geochem. 42(9), 1055-1064.

Inagaki, T.M, Possinger, A.R., Grant, K.E., Schweizer, S.A., Mueller, C.W., Derry, L.A., Lehmann, J., Kögel-Knabner, I., 2020. Subsoil organo-mineral associations under contrasting climate conditions. Geochim. Cosmochim. Acta 270, 244-263.

Knicker, H., Lüdemann H.D., 1995. N-15 and C-13 CPMAS and solution NMR studies of N-15 enriched plant material during 600 days of microbial degradation. Org. Geochem. 23, 329-341.

Kurtz, A.C., Derry, L.A., Chadwick, O.A., Alfano, M.J., 2000. Refractory element mobility in volcanic soils. Geology 28(8), 683-686.

Parfitt, R.L., Childs, C.W., 1988. Estimation of forms of Fe and Al: A review, and analysis of contrasting soils by dissolution and Mossbauer methods. Aust. J. Soil. Res. 26, 121-144.

Preston, C.M., Dudley, R.L., Fyfe, C.A., Mathur, S.P., 1984. Effects of variations in contact times and copper contents in a ^{13}C CPMAS NMR study of samples of four organic soils. Geoderma 33, 245-253.

Ravel, B, Newville, M., 2005. Athena, Artemis, Hephaestus: data analysis for X-ray absorption spectroscopy using IFEFFIT. J. Synchrotron Rad. 12, 537-541.

Ross, G.J., Wang, C., 1993. Extractable Al, Fe, Mn, and Si, in: Carter, M.R (Ed.), Soil Sampling and Methods of Analysis. Canadian Society of Soil Science, Lewis Publishers, Boca Raton, pp. 239-246.

Shang, C., Zelazny, L.W., 2008. Selective dissolution techniques for mineral analysis of soils and sediments, in: Ulery, A.L., Drees, L.R. (Eds.), Methods of Soil Analysis, Part 5, Mineralogical Methods. SSSA Book Series No. 5. Soil Science Society of America, Madison, WI, pp. 33-80.

Solomon, D., Lehmann, J., Kinyangi, J., Liang, B., Heymann, K., Dathe, L., Hanley, K., Wirick, S., Jacobsen, C., 2009. Carbon (1s) NEXAFS spectroscopy of biogeochemically relevant reference organic compounds. Soil Sci. Soc. Am. J. 73, 1817-1830.

Wojdyr, M., 2010. Fityk: a general-purpose peak fitting program. J. Appl. Cryst. 43, 1126-1128.

Supplementary Tables

Supplementary Table A1. Field descriptions of sampling locations for typical, Bhs, and E podzols, associated with low, medium, and high saturation frequency soils, respectively.

Podzol type	Profile	Latitude (decimal degrees)	Longitude (decimal degrees)	Aspect (degrees)	Slope (up) (%)	Slope (down) (%)	Physio-graphy	Land shape	Depth to water table (m)	Depth to redox (m)
Typical (low sat. freq.)	A	43.955533	-71.718826	266	26	30	Backslope	Nose	>1.07	0.30
	B	43.955475	-71.718810	266	26	30	Backslope	Nose	0.97	0.97
	C	43.955513	-71.718896	266	26	30	Backslope	Nose	0.90	0.73
Bhs (medium sat. freq.)	A	43.956993	-71.717263	242	18	15	Shoulder	Hollow foot	0.74	0.48
	B	43.956601	-71.717530	250	23	28	Upper backslope	Hollow	0.28	0.37
	C	43.956620	-71.717481	251	27	26	Not recorded	Hollow	Not recorded	Not recorded
E (high sat. freq.)	A	43.956623	-71.717486	230	56	22	Backslope	Hollow foot	0.21	NA
	B	43.956998	-71.717241	242	18	15	Shoulder	Hollow foot	0.43	0.31
	C	43.956976	-71.717225	242	18	15	Shoulder	Hollow foot	0.35	0.15

Supplementary Table A2. Field soil profiles descriptions for summarized by hydropedological units (typical, Bhs, and E) corresponding to low, medium, and high saturation frequency soils, showing ranges of properties for three replicate profiles. Abbreviations: Texture: SL = sandy loam, LS = loamy sand; Structure: GR = granular, SBK = sub-angular blocky, M = massive; Consistence: FR = friable, FI = firm, VFR = very friable, VFI = very firm; Roots: M = many, C = common, F = few, A = absent.

		Horizon ID	Top (m)	Bottom (m)	Matrix color range	Texture	Structure	Consistence	Coarse (%)	Roots
Typical	1,2	Oi, Oe	0	0.05-0.11	NA	NA	NA	NA	NA	NA
	3	Oa	0.03-0.11	0.07-0.22	2.5YR-7.5YR 2.5/1	NA	GR	VFR, FR	0	M
	4	E	0.09-0.22	0.11-0.32	10YR 5/2	SL	GR/SBK	FR	2-7	C
	5	Bhs/Bhs1	0.11-0.32	0.14-0.40	5YR 2.5/1-2.5/2	SL	SBK	FR	2-5	C
	6	Bs/Bhs2	0.14-0.40	0.20-0.60	5YR 3/4-7.5YR 2.5/3	SL	SBK	FR	2-5	F/C
	7	Bs/BC1/Bh	0.20-0.60	0.30-0.73	7.5YR 3/4-10YR 4/4	SL	SBK	FR	2-5	F/C
	8	BC1/BC2/CB	0.30-0.73	0.67-0.90	10YR 3/4-2.5Y 5/3	SL	SBK	FR/FI	3-10	F/C
	9	BC2/CB/Cd	0.67-0.90	0.98-1.02	10YR 4/4-2.5Y 6/2	SL/LS	SBK/M	FR/FI	5-7	F/A
	10	Cd	0.97-1.02	1.07+	2.5Y 5/2-5/3	LS	M	FI/VFI	7-8	F/A
Bhs	1,2	Oi. Oe	0	0.06-0.07	NA	NA	NA	NA	NA	NA
	3	Oa/Oa1	0.06-0.07	0.11-0.18	2.5YR 6/1-7.5YR2.5/1	NA	GR	VFR	0	M
	4	E/Bhs1/Oa2	0.11-0.18	0.17-0.37	7.5YR 2.5/1-5/2	SL	GR/SBK	VFR/FR	0-4	M/C/F
	5	Bhs/Bhs1/Bhs2	0.17-0.37	0.26-0.55	5YR 2.5/2-7.5YR 3/2	SL	SBK	FR/FI	3-5	F/M
	6	Bhsm/BC/Bhs1	0.26-0.55	0.47-0.74	2.5Y 5/3-7.5YR 3/3	SL	SBK	FI/FR	5-10	C/F/A
	7	Bhs3/Cd	0.47-0.74	0.78-0.96	7.5YR 3/2	SL	SBK	FR	5	F
	8	CB	0.96	1.21+	2.5Y 4/2	SL	M	FR	5	A
E	1,2	Oi, Oe	0	0.05	NA	NA	NA	NA	NA	NA
	3	Oa/Oa1	0.05	0.10-0.15	5YR 2.5/1-7.5YR 2.5/1	NA	GR	VFR	0-2	M
	4	E/Oa2	0.10-0.15	0.17-0.35	7.5YR 4/2-5YR 2.5/1	SL/LS	GR/SBK	FR/VFR	5-8	F/M
	5	Bs/E1/R	0.17-0.35	0.31-0.45	10YR 5/1-7.5YR 3/4	SL/LS	SBK	FR	3-7	F/A
	6	E2/R	0.31-0.45	0.38	10YR 3/1	SL	SBK	FI	5	F
	7	Bhs	0.38	0.43	7.5YR 7.5/1	SL	SBK	FI	8	F
	8	CB	0.43	0.57	2.5 4/2	SL	M	VFI	5	A
	9	R	0.57+	NA	NA	NA	NA	NA	NA	NA

Supplementary Table A3. Tree (>0.1 m diameter at breast height (DBH)) species identification for hydropedological units (HPU) sampling sites (310 m^2 survey area). Sampling locations and HPU assignments are shown in Supplementary Fig. A1.

HPU	Species	Common name	Basal area (m^2 ha^{-1})
Typical	*Fagus grandifolia*	American beech	1.60
	Acer pensylvanicum	Striped maple	1.06
	Acer saccharum	Sugar maple	6.87
	Betula alleghaniensis	Yellow birch	11.73
Bhs/E	*Fagus grandifolia*	American beech	1.23
	Abies balsamea	Balsam fir	5.68
	Picea rubens	Red spruce	0.59
	Acer pensylvanicum	Striped maple	1.12
	Acer saccharum	Sugar maple	1.64
	Betula papyrifera	White birch	6.94
	Betula alleghaniensis	Yellow birch	12.62
E/Bhs	*Abies balsamea*	Balsam fir	3.41
	Picea rubens	Red spruce	9.02
	Acer pensylvanicum	Striped maple	5.30
	Betula papyrifera	White birch	0.58
	Betula alleghaniensis	Yellow birch	17.23

Supplementary Table A4. List of sample subsets used for (1) incubation, (2) X-ray spectroscopy and hydroxylamine OC extraction, and (3) nuclear magnetic resonance iron interference experiments.

	Saturation Frequency	Profile	Horizon	C content after macro-POM removal (%)
Incubation	Low	A	Bhs1	9.94
	Medium	B	Bhs1	3.47
	High	B	Bhs	1.29
Fe K-edge and C K-edge XAS, hydroxylamine OC experiment	Low	A	Bhs1	
	Low	B	Bhs1	
	Low	C	Bhs	
	Medium	A	Bhs	
	Medium	B	Bhs1	
	Medium	C	Bhs1	
	High	B	Bhs	
	High	B	BC	
	High	C	Bs	
NMR Fe interference experiment	Low	A	Bhs1	
	Low	B	Bhs2	
	Low	C	Bh	
	Medium	A	Bhs	
	Medium	B	Bhs1	
	High	B	Bhs	

Supplementary Table A5. Average (± standard deviation) bulk characterization data for mineral soils from eluvial (E), spodic (Bhs/Bh/Bs), transitional (BC/CB), and substratum (Cd) horizons collected from typical, Bhs, and E podzol hydropedological soil units with low, medium, and high saturation frequency, respectively. NA = not applicable (no standard deviation, n = 1). Volumetric water content was determined for soils at the time of sampling.

Saturation Frequency	Horizon	pH	Volumetric water content	Total C	Total N	Total Fe	Total Al	Total Mn
			$m^3\ m^{-3}$			$g\ kg^{-1}$ dry soil		
Low	Eluvial (n=3)	3.1 ±0.1	22.3 ±3.0	12.9 ±5.6	0.71 ±0.27	6.4 ±0.5	42.6 ±3.4	0.29 ±0.031
	Spodic (n=8)	3.7 ±0.3	35.8 ±2.8	60.6 ±10.9	2.41 ±0.56	25.7 ±7.0	52.9 ±7.9	0.28 ±0.087
	Transitional (n=6)	4.2 ±0.1	31.4 ±5.3	23.5 ±9.2	0.96 ±0.34	17.0 ±3.4	57.6 ±3.3	0.273.3 ±0.057
	Substratum (n=3)	4.5 ±0.1	19.8 ±1.1	3.6 ±0.9	0.18 ±0.024	15.9 ±0.6	60.5 ±1.5	0.31 ±0.061
Medium	Eluvial (n=1)	4.0 NA	33.8 NA	9.9 NA	0.53 NA	5.6 NA	40.2 NA	0.36 NA
	Spodic (n=7)	3.9 ±0.2	45.1 ±10.9	45.7 ±27.2	1.97 ±1.41	25.7 ±4.7	58.5 ±2.0	0.40 ±0.086
	Transitional (n=1)	4.0 NA	29.6 NA	16.2 NA	0.59 NA	20.1 NA	59.5 NA	0.55 NA
High	Eluvial (n=4)	4.0 ±0.2	29.7 ±1.6	8.0 ±2.2	0.42 ±0.076	6.0 ±1.7	50.0 ±5.5	0.37 ±0.098
	Spodic (n=2)	4.3 ±0.1	33.8 ±7.0	12.4 ±1.5	0.46 ±0.046	12.6 ±1.7	52.2 ±2.4	0.35 ±0.063
	Transitional (n=1)	4.5 NA	34.4 NA	15.2 NA	0.59 NA	26.6 NA	69.2 NA	0.420 NA

Supplementary Table A6. Average (± standard deviation) selective metal extraction values, presented as proportion of total metal content for each iron (Fe), aluminum (Al), and manganese (Mn). Abbreviations: ODOE = optical density of oxalate extract, Abs = absorbance (a.u.), H = hydroxylamine-hydrochloric acid (HCl)-extractable, O = acid ammonium oxalate-extractable, D = citrate-dithionite extractable. NA = not applicable (no standard deviation, n = 1).

Saturation Frequency	Horizon	ODOE	Fe-O	Al-O	Mn-O	Fe-D	Al-D	Fe-H	Al-H	Mn-H
		Abs				(% total)				
Low	Eluvial (n=3)	0.1 ±0.1	27.9 ±5.1	1.4 ±0.6	1.7 ±0.3	31.1 ±4.7	0.9 ±0.4	19.7 ±6.4	1.7 ±0.7	2.9 ±0.5
	Spodic (n=8)	1.7 ±0.7	67.0 ±19.2	23.2 ±7.3	4.1 ±1.1	66.1 ±14.2	18.2 ±5.2	46.8 ±13.1	23.3 ±8.1	6.4 ±2.7
	Transitional (n=6)	0.4 ±0.2	30.9 ±13.3	17.2 ±6.4	4.8 ±2.7	35.1 ±14.5	11.8 ±4.7	24.6 ±6.9	18.6 ±6.5	7.8 ±2.6
	Substratum (n=3)	0.04 ±0.0	12.0 ±2.6	6.3 ±0.3	21.8 ±16.2	14.8 ±1.0	3.3 ±0.4	15.5 ±1.9	7.7 ±0.5	26.0 ±15.6
Medium	Eluvial (n=1)	0.2 NA	48.4 NA	2.6 NA	1.2 NA	38.0 NA	1.5 NA	37.4 NA	3.6 NA	2.2 NA
	Spodic (n=7)	0.7 ±0.2	68.3 ±10.9	12.7 ±3.5	2.7 ±1.7	65.6 ±8.4	10.5 ±2.9	54.9* ±7.1	12.7* ±3.7	4.7 ±2.0
	Transitional (n=1)	0.4 NA	39.3 NA	7.9 NA	0.6 NA	36.7 NA	6.0 NA	37.6 NA	9.4 NA	3.9 NA
High	Eluvial (n=4)	0.2 ±0.3	17.2 ±9.4	2.4 ±1.7	0.6 ±0.3	20.4 ±9.6	1.6 ±1.4	16.9 ±7.0	2.9 ±1.6	1.9 ±1.0
	Spodic (n=2)	0.2 ±0.2	44.1 ±3.0	8.1 ±2.5	0.9 ±0.2	43.3 ±1.1	6.2 ±1.5	35.9 ±1.5	8.4 ±2.8	2.7 ±0.3
	Transitional (n=1)	0.1 NA	39.1 NA	13.6 NA	3.1 NA	36.1 NA	9.4 NA	32.5 NA	13.8 NA	6.8 NA

*N=6

Supplementary Table A7. Iron K-edge X-ray absorption near-edge structure (XANES) results for soil samples and standards. Edge position, white line, and pre-edge centroid are shown for normalized fluorescent (μE). The 7120.0 eV peak area is determined for the first derivative μE. Standard compound XANES data are also included in Inagaki et al. (2020).

	Soil Samples			Fe(III) minerals		Fe(III)/(II) mineral	Fe(II) mineral	Fe(III)-organic complex		Fe(II)-organic
	Low (Typical)	Medium (Bhs)	High (E)	Goethite	Ferrihydrite	Fe(II)-nontronite	Fayalite	Fe (III) citrate	Fe (III) EDTA	Fe (II) citrate
Edge (E_0) (eV)	7127.3 (0.6)	7126.3 (2.1)	7125.0 (1.7)	7123	7127	7124	7123	7125	7126	7124
White line (eV)	7132.0 (0.0)	7131.7 (0.6)	7131.0 (0.0)	7131	7133	7131	7127	7134	7134	7126
Pre-edge centroid (eV)	7114.3 (0.6)	7114.3 (0.6)	7114.7 (0.6)	7114	7114	7113	7112	7114	7113	7113
7120.0 peak area (%)	10.14 (2.8)	14.32 (7.9)	21.90 (3.4)	3.17	1.28	22.10	63.13	11.81	7.57	39.43

Supplementary Table A8. Carbon K-edge near-edge X-ray absorption fine structure peak energy positions (eV) and height (normalized to edge step = 1) for average (n = 3 horizons, ± standard deviation in brackets only for bulk soils) spodic horizon bulk soils, soils used for incubation studies with macro (> 125μm) particulate organic matter (POM) removed, and water-extractable organic matter derived from incubation soils.

		Aromatic (C=C)		Substituted aromatic (C=C-OH)		Carboxylic (C=O)	
Sample Type	Saturation Frequency	Peak centroid (eV)	Normalized peak height (a.u.)	Peak centroid (eV)	Normalized peak height (a.u.)	Peak centroid (eV)	Normalized peak height (a.u.)
Bulk spodic horizons soils	Low	285.7 (0.2)	0.50 (0.03)	286.7 (0.1)	0.47 (0.02)	288.8 (0.1)	0.70 (0.02)
	Medium	285.8 (0.1)	0.39 (0.06)	286.8 (0.0)	0.41 (0.04)	288.7 (0.0)	0.71 (0.02)
	High	285.6 (0.1)	0.28 (0.03)	286.8 (0.0)	0.31 (0.04)	288.8 (0.1)	0.73 (0.04)
Macro-POM removed	Low	285.7	0.50	286.8	0.50	288.8	0.75
	Medium	285.5	0.29	286.8	0.35	288.8	0.70
	High	285.7	0.32	286.8	0.33	288.9	0.72
Water-extractable organic matter	Low	285.6	0.34	286.8	0.40	288.8	0.74
	Medium	285.6	0.27	286.9	0.34	288. 8	0.75
	High	285.6	0.33	286.9	0.31	288.9	0.82

Supplementary Figures

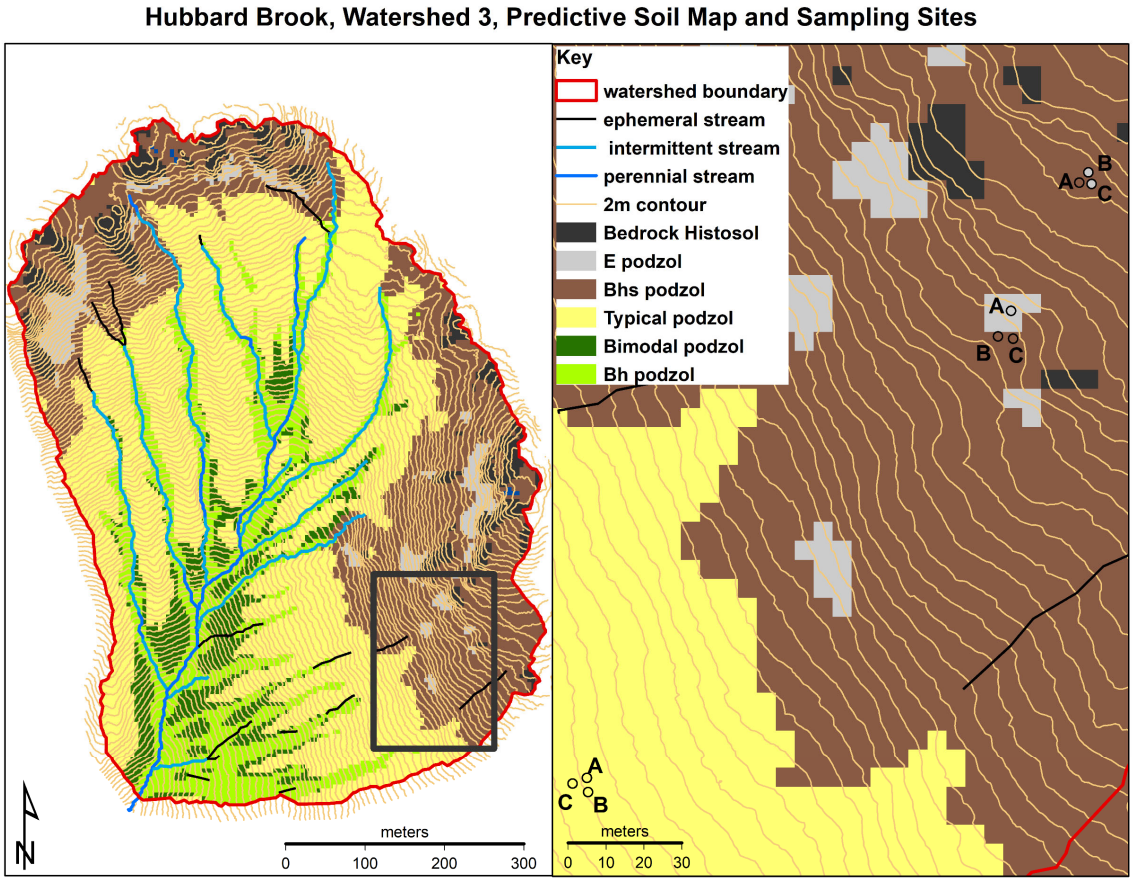

Supplementary Figure A1. Map of Watershed 3, Hubbard Brook Experimental Forest, Woodstock, New Hampshire. Predicted locations of hydropedological units (HPUs) used to locate soil units associated with saturation cycle frequency categories are shown in the left panel, where Typical = low, Bhs = medium, and E = high saturation cycle frequency (defined by the number of saturated-unsaturated cycles in the upper B horizon), respectively. Soil units located at lower elevations and at the watershed boundary (Bimodal, Bh, and Bedrock Histosol) were not sampled in this study. The right panel shows detail of the area sampled in the study, with individual soil pits (A, B, and C for each soil type) colored by actual HPU designation based on diagnostic profile characteristics (see Figure 1) determined in the field.

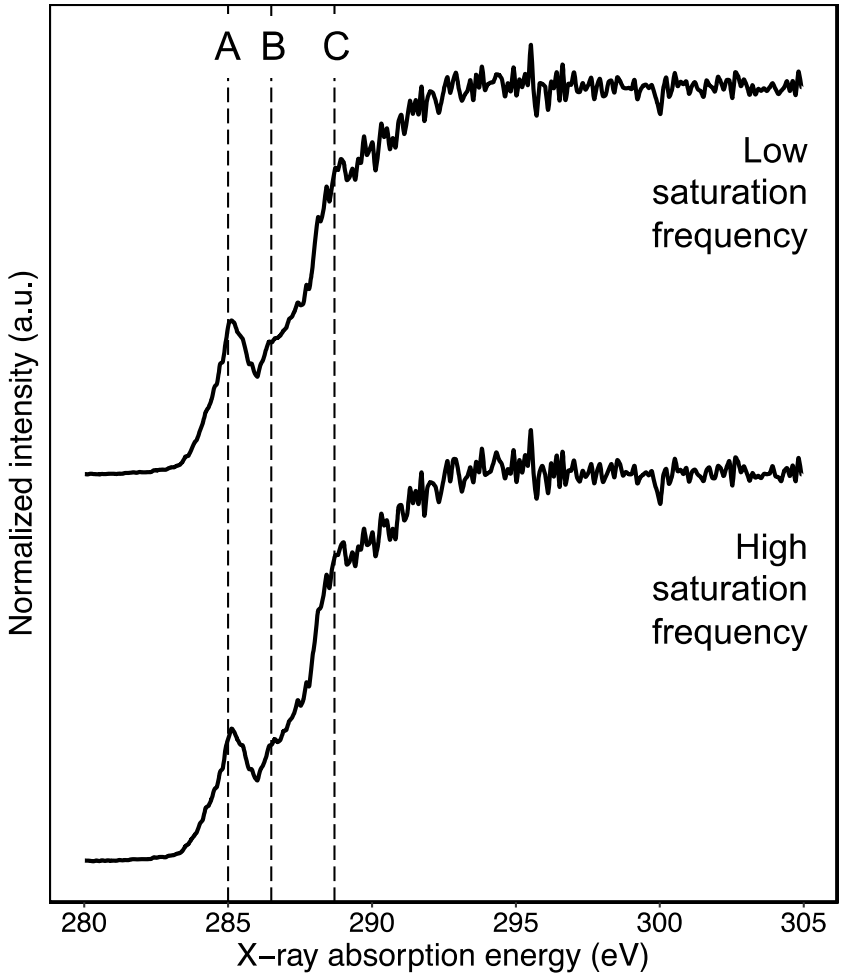

Supplementary Figure A2. Carbon (C) K-edge X-ray absorption fine structure (XANES) spectra for organic (Oa) horizon water-extractable organic matter from soil units with high and low saturation cycle frequency (defined by the number of saturated-unsaturated cycles in the upper B horizon). Spectra are shown normalized to edge step = 1 and unsmoothed. Vertical lines A, B, and C indicate aromatic (285.0 eV), substituted aromatic (286.5 eV), and carboxylic (288.7 eV) features, respectively.

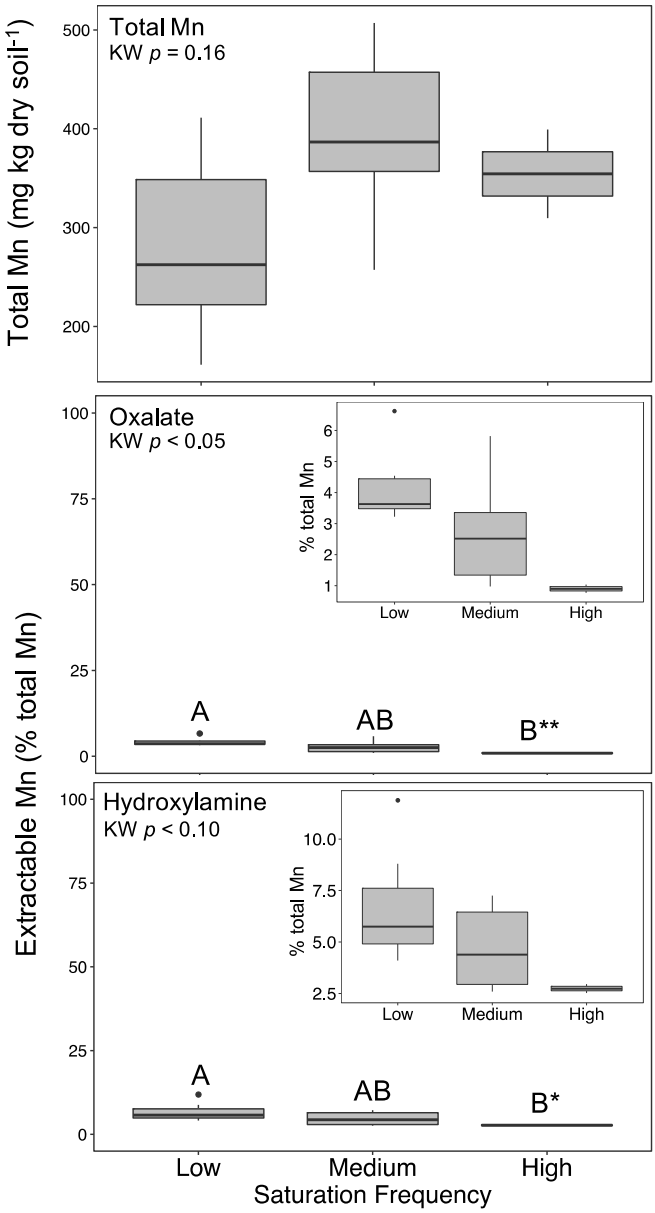

Supplementary Figure A3. Bulk soil total and extractable manganese (Mn) for spodic horizons of low (n = 8), medium (n = 7), and high (n = 2) saturation frequency soils (defined by the number of saturated-unsaturated cycles in the upper B horizon). Within each extractant, *p*-values are shown for overall Kruskal-Wallis ANOVA on ranks. Letters show post-hoc multiple comparisons (Dunn Test with Bonferroni correction), with different letters showing significant differences at α = 0.1 (*) and α = 0.05 (**). Lower and upper edges of boxes show first and third quartiles (25th and 75th percentiles) and lower and upper whiskers show the smallest and largest value no further than 1.5*interquartile range (IQR) of the box edges. Individual points beyond whiskers are considered outliers. Inset boxes show same data with adjusted Y-axis scale

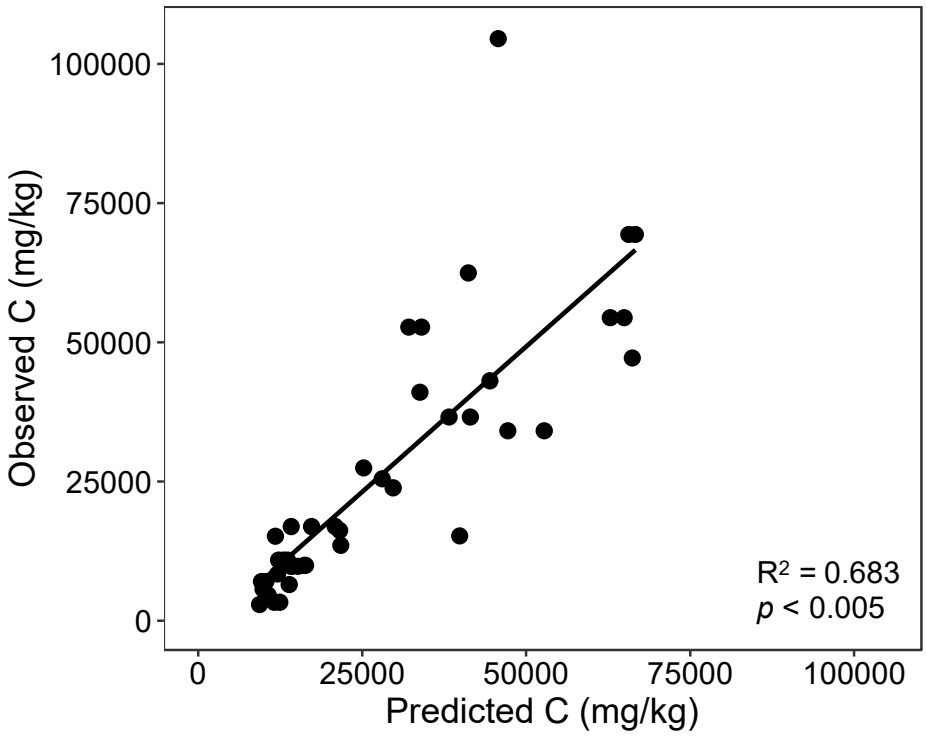

Supplementary Figure A4. Random Forest regression predicted (model-derived) and observed (testing set) values of total C. Point data show repeated (n=5) independent iterations of the regression model, fit by linear regression with the shaded region showing standard error.

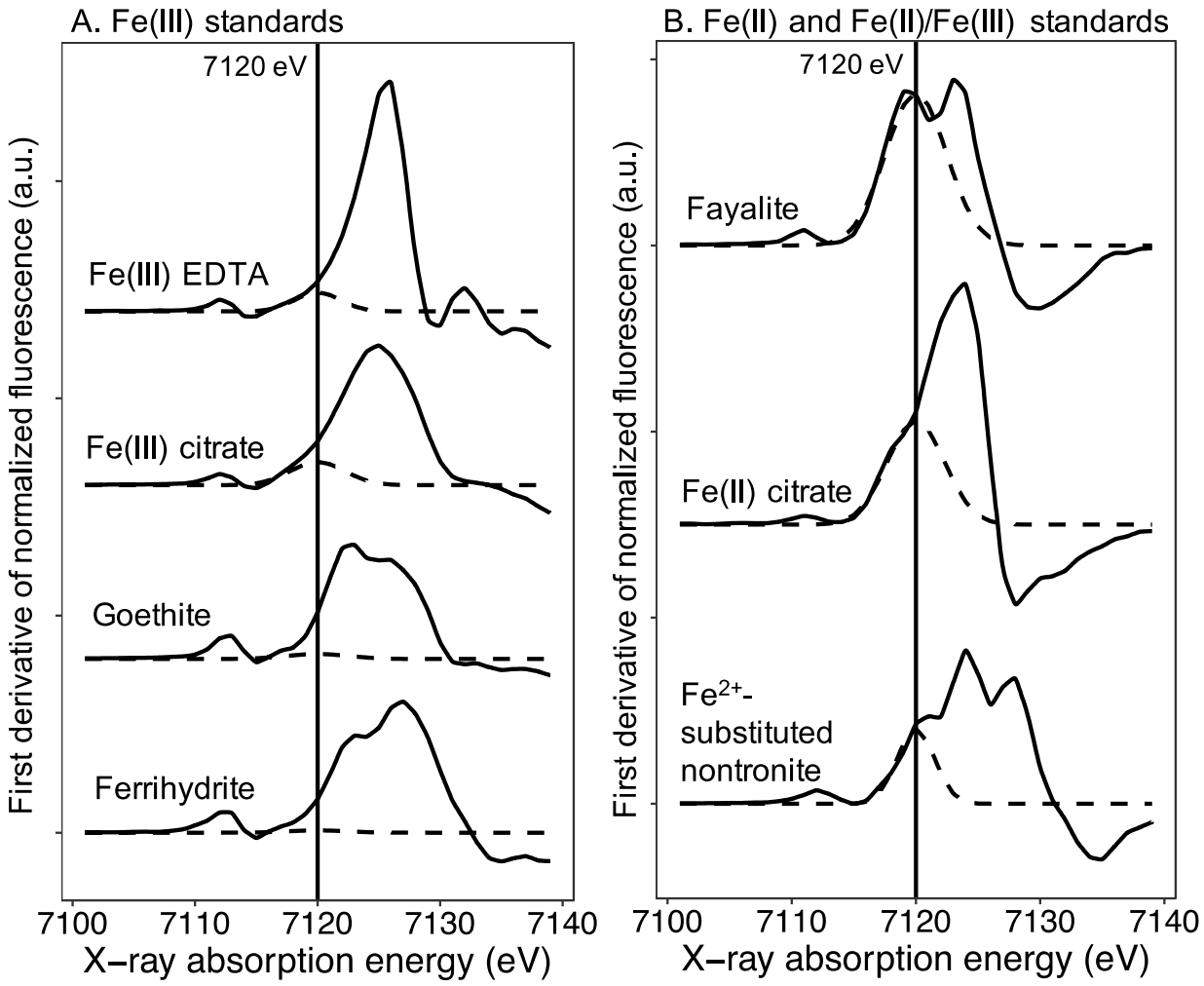

Supplementary Figure A5. Iron K-edge X-ray absorption near-edge structure (XANES) first derivative of normalized fluorescence intensity ($dx/d\mu(E)$). The feature at 7120.0 eV (vertical line) is associated with the 1s-4s Fe K-edge transition (Berry et al., 2003) and is used as a proxy for increasing contribution of reduced Fe(II). Standard spectra show an increasing contribution of 7120 eV area from oxidized Fe mineral standards (**A**) compared to reduced Fe mineral standards (**B**). Reference spectra are also included in Inagaki et al. (2020) (Appendix A).

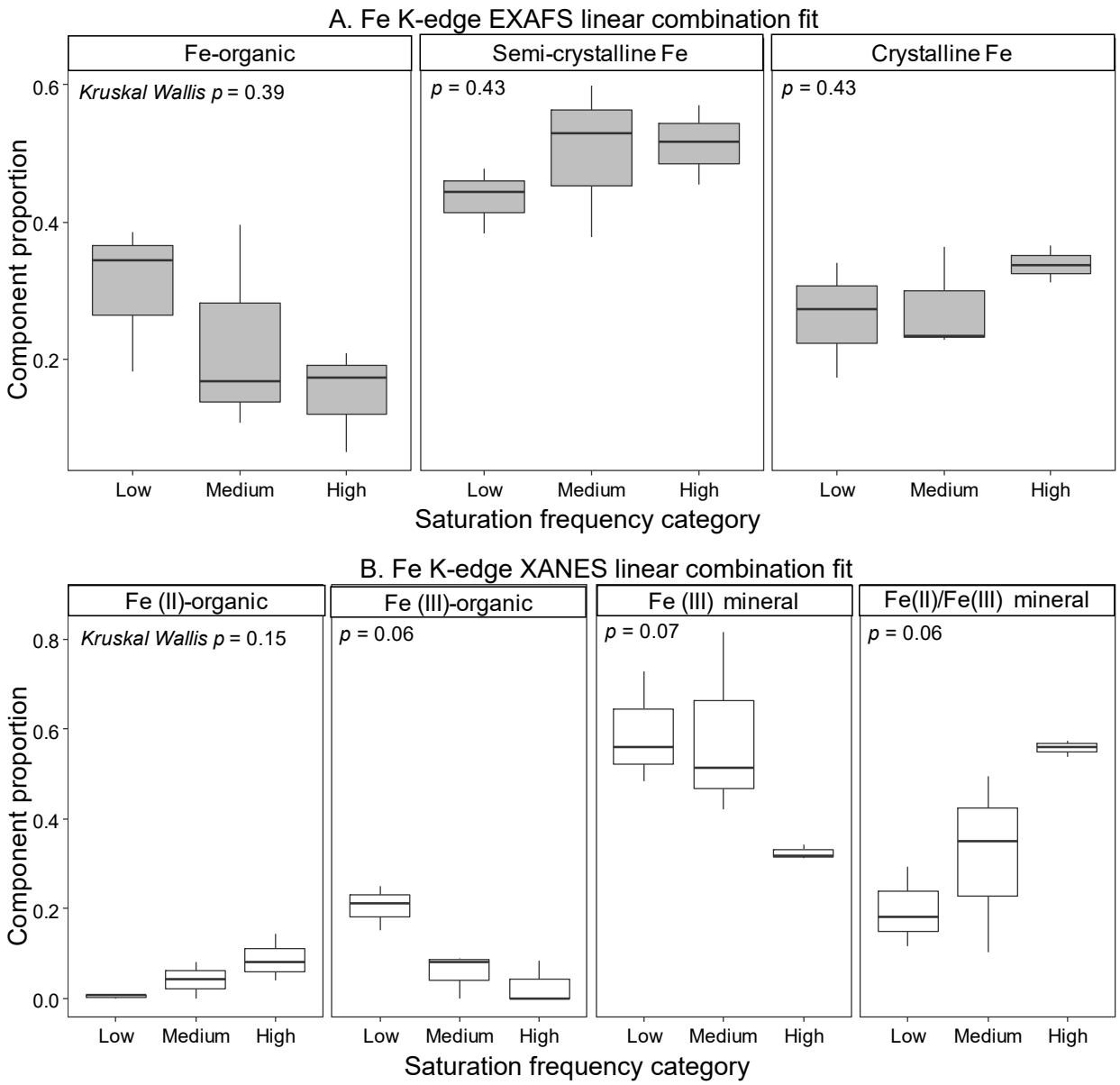

Supplementary Figure A6. Iron (Fe) K-edge extended X-ray absorption fine structure (EXAFS) (**A**) and X-ray absorption near-edge structure (XANES) linear combination fit (LCF) results for soils of varying saturation cycle frequency (defined by the number of saturated-unsaturated cycles in the upper B horizon) (**B**). Boxplots show the distribution of fit results for spodic/transitional horizons (n = 3 for each saturation frequency) (horizons listed in Supplementary Table A4). Lower and upper edges of boxes show first and third quartiles (25th and 75th percentiles) and lower and upper whiskers show the smallest and largest value no further than 1.5*interquartile range (IQR) of the box edges. Within each component, *p*-values are for Kruskal-Wallis ANOVA on Ranks.

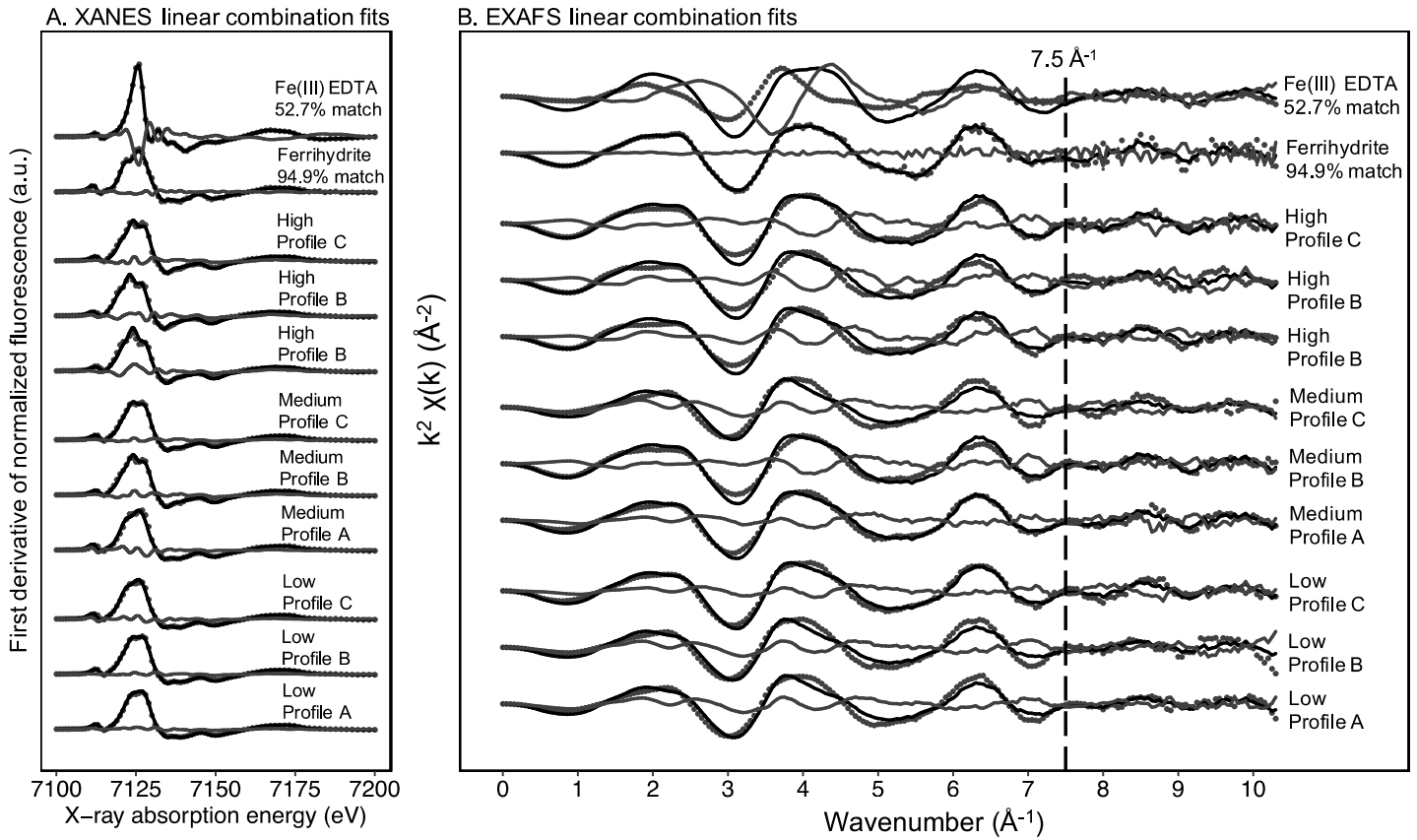

Supplementary Figure A7. Linear combination fits for iron (Fe) K-edge X-ray absorption near-edge structure (XANES) (**A**) and extended X-ray absorption fine structure (EXAFS) (**B**) for replicate spodic/transitional horizons from low, medium, and high saturation frequency soil profiles (listed in Supplementary Table A4).Points show raw data, with the black curve showing the LCF best fit and grey line LCF residuals. For EXAFS (**B**), the feature at 7.5 $Å^{-1}$ is associated with outer-shell Fe bonding and is increased with decreasing Fe-organic bonding (Chen et al., 2014), most prominently in high saturation frequency sample B. For standards, LCF fitting procedures were applied to determine the accuracy of matching similar compounds; for XANES, Fe(III) EDTA matched 100% to Fe(III) citrate, and ferrihydrite matched 97.5% to ferrihydrite synthesized separately. For EXAFS, Fe(III) EDTA matches poorly to Fe(III) citrate (54.7%), mainly due to mismatch in the lower wavenumber region, but best represents the feature at 7.5 $Å^{-1}$ highlighted and was consequently used for LCF. Ferrihydrite was similarly accurate to XANES LCF at 94.9% match.

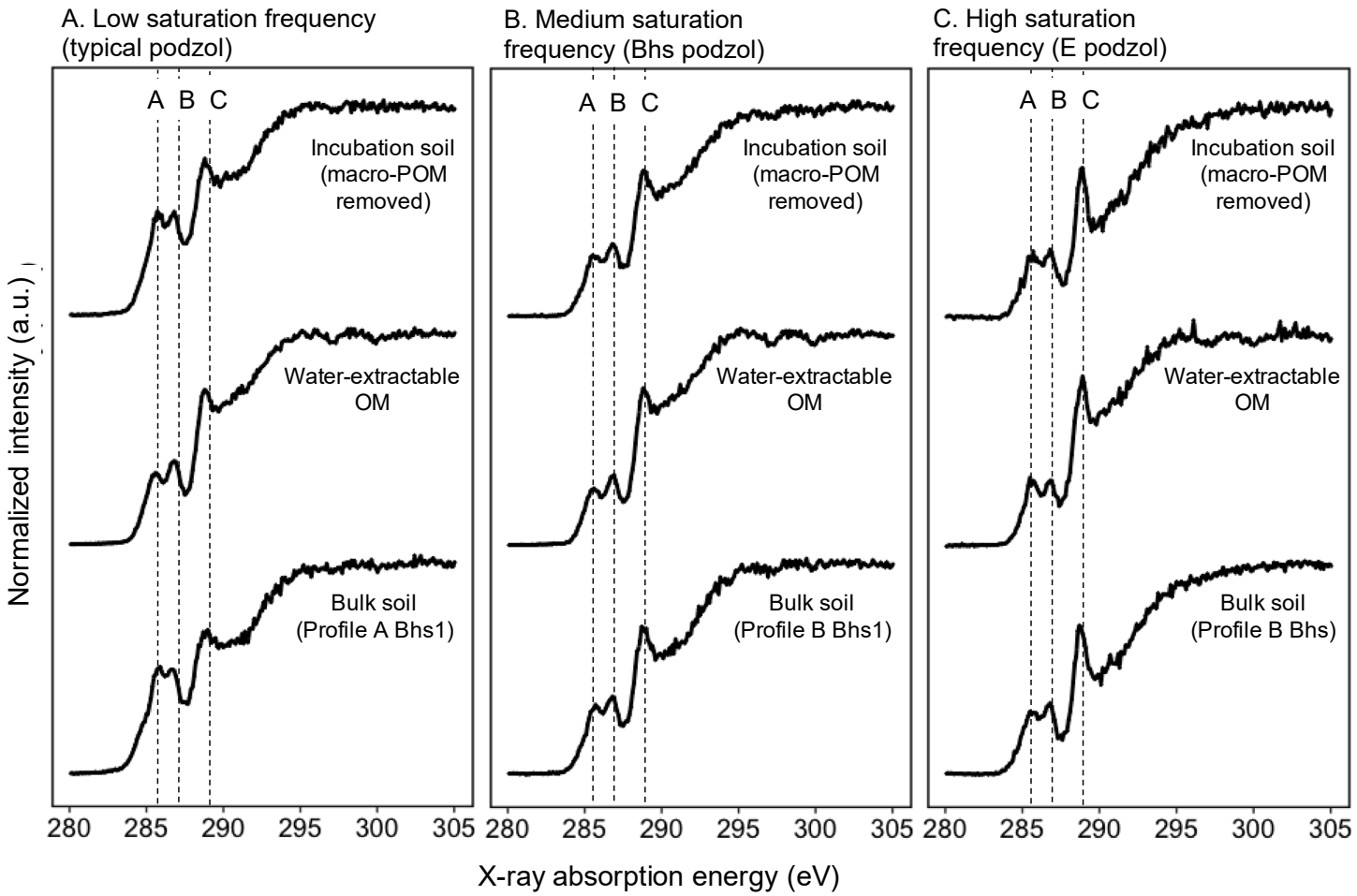

Supplementary Figure A8. Carbon (C) K-edge X-ray absorption fine structure (XANES) spectra for bulk soils with varying saturation frequency categories compared to water-extractable organic matter (WEOM) and macro-particulate organic matter (POM) removed. Spectra are shown normaled to edge step = 1 and unsmoothed. Vertical lines A, B, and C indicate aromatic (~285.0 eV), substituted aromatic (~286.5 eV), and carboxylic (~288.7 eV) features, respectively.

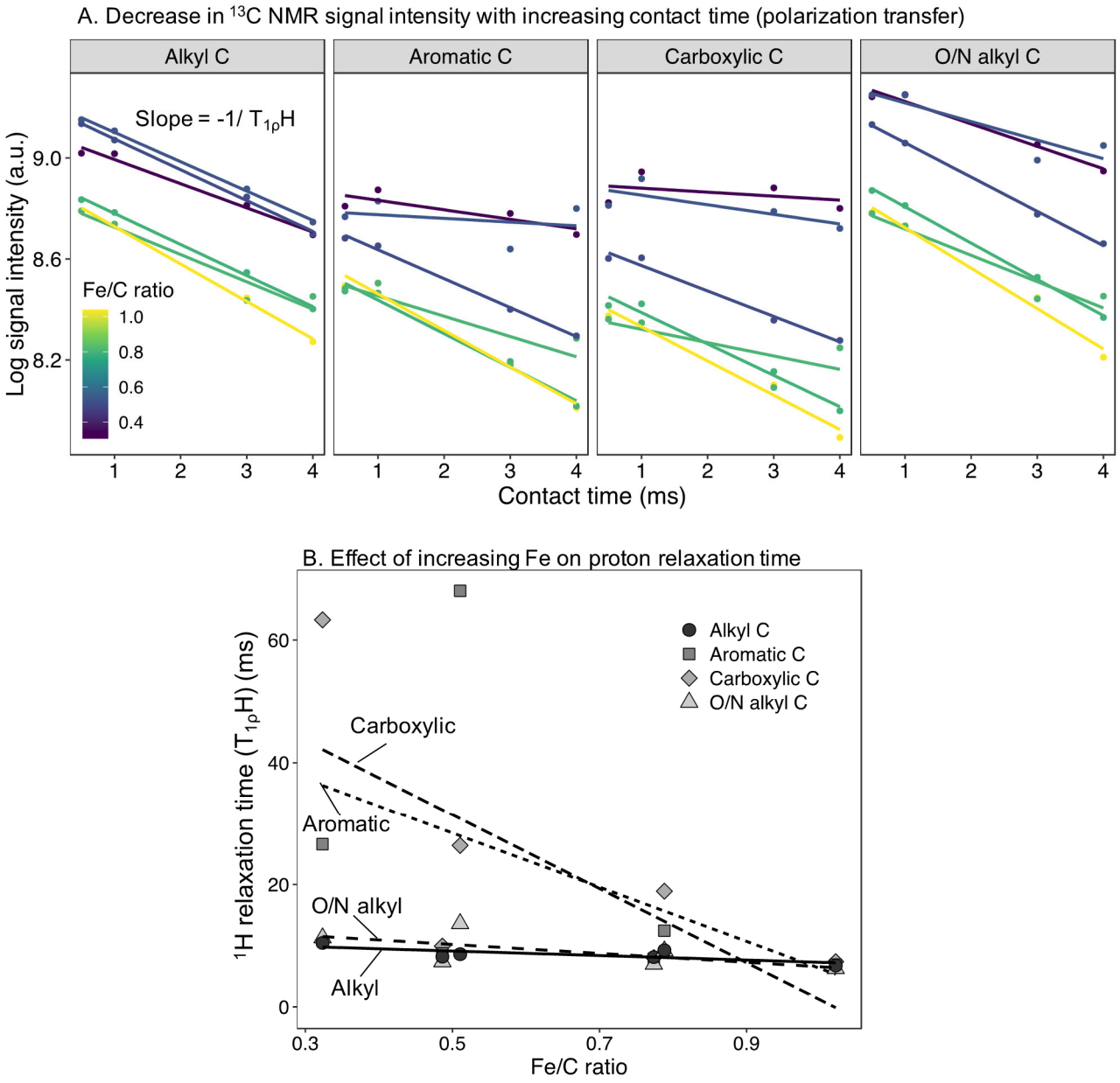

Supplementary Figure A9. **A**. Decrease in ^{13}C NMR log(signal intensity) as a function of contact time for soil samples with increasing total carbon (C) to total iron (Fe) ratios. All saturation frequency categories are pooled due to limited sample number for high saturation frequency (n=1). **B**. Proton relaxation time ($T_{1\rho}$H) as a function of increasing iron (Fe) content (increasing Fe/C ratio). A significant difference in the effect of Fe/C on relaxation time was detected among carbon forms (multiple linear regression F-test $p <$ 0.1), with a stronger Fe(III) interference (relaxation time shortening) for carboxylic and aromatic C compared to alkyl and O/N alkyl C. Due to low sample numbers, soils with different saturation frequency are not considered separately for this analysis.

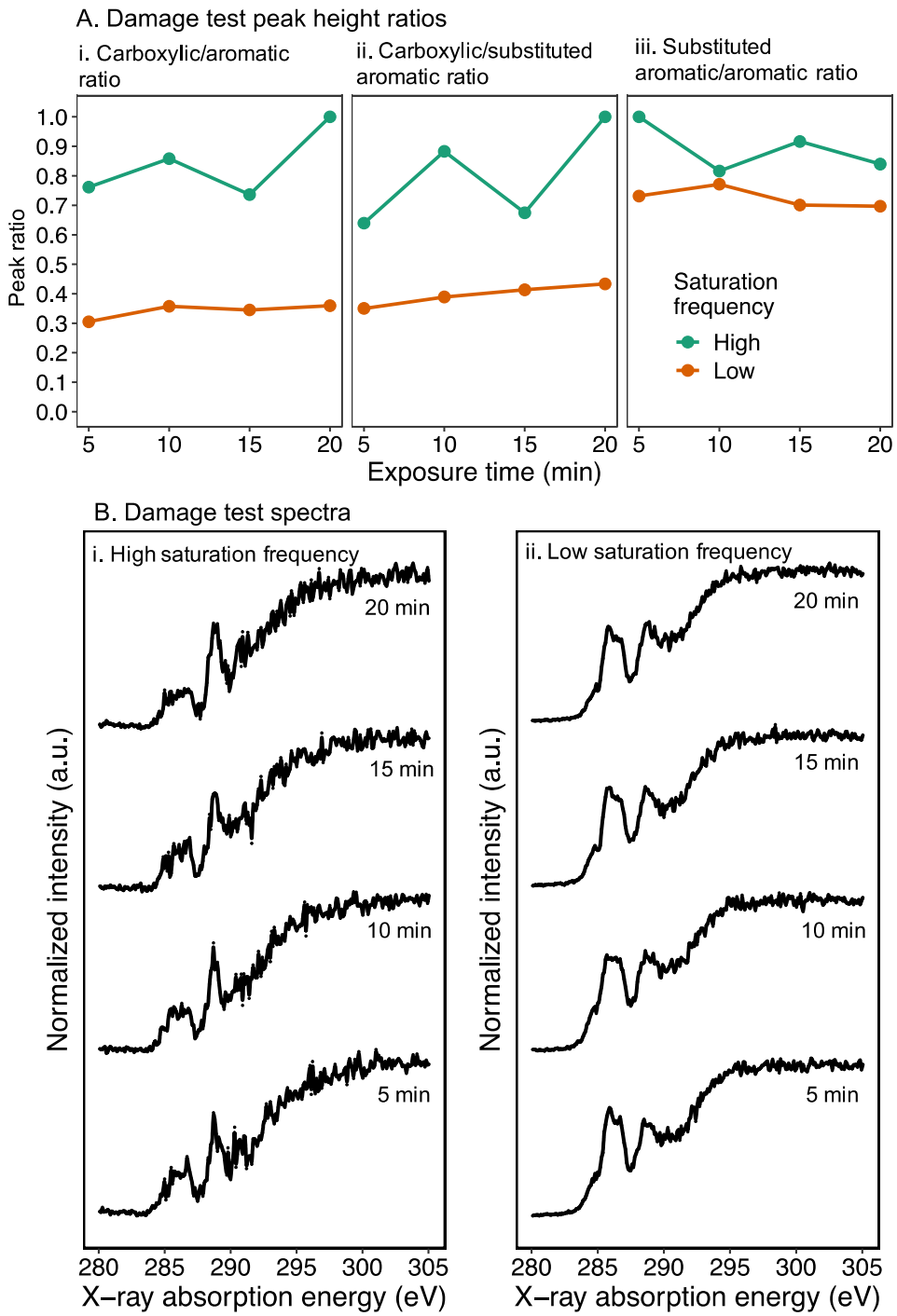

Supplementary Figure A10. Damage test assessment for carbon (C) K-edge near-edge X-ray absorption fine structure. The change in carboxylic/aromatic (**A.i**), carboxylic/substituted aromatic (**A.ii**), and substituted aromatic/aromatic (**A.iii.**) C shows variation over time but lacks a strong direction trend associated with the large increase in dwell time. The spectra used to derive ratios are shown for high (**B.i**.) and low (**B.ii**.) saturation frequency, normalized to edge step=1 and unsmoothed.